Hardening mechanisms of high pressure Mg-Li alloys

Qiuming Peng, Wenshi Wu, Jianxin Guo, Jianyong Xiang, and S. S. Zhao

Citation: Journal of Applied Physics **115**, 023511 (2014); doi: 10.1063/1.4861631
View online: http://dx.doi.org/10.1063/1.4861631
View Table of Contents: http://scitation.aip.org/content/aip/journal/jap/115/2?ver=pdfcov
Published by the AIP Publishing

Hardening mechanisms of high pressure Mg-Li alloys

Qiuming Peng,[a] Wenshi Wu, Jianxin Guo, Jianyong Xiang, and S. S. Zhao
State Key Laboratory of Metastable Materials Science and Technology, Yanshan University, Qinhuangdao 066004, People's Republic of China

(Received 9 October 2013; accepted 23 December 2013; published online 10 January 2014)

High pressure thermal-mechanical treatment (4 GPa) is introduced to improve hardness of a Mg-7 wt. % Li alloy. The improvement in hardness is strongly temperature dependent and the highest hardness occurs in a narrow temperature range around 700 °C. The main reasons for improved hardness are mainly related to the increased phase relative abundance of hcp phase and the formation of superfine $\{10\bar{1}1\}$ compression twins in hcp-$Li_{0.92}Mg_{4.08}$ phase which effectively inhibits dislocation movement during deformation process. This phase transformation is consistent with the first principles calculations. It demonstrates that high pressure treatment is an effective approach to achieve higher strength Mg-Li based materials © *2014 AIP Publishing LLC*. [http://dx.doi.org/10.1063/1.4861631]

I. INTRODUCTION

More recently, high pressure (HP) has attracted extensive attentions because it is one of effective techniques to prepare new compounds or to obtain unique properties. The hardness and toughness of nanotwinned cubic BN synthesized under super HP (25 GPa) are better than those of natural diamond.[1] A new hydride of MgY_2H_y with fcc structure has been prepared at 850 °C under 3 GPa in Mg-Y-H system.[2] In addition, a Al-32 wt. % Mg alloy solidified under 3 GPa has remarkably improved ultimate tensile strength.[3] It is demonstrated that exterior pressure plays an essential role in phase formation and its transformation, especially reaching the scale of GPa. Therefore, it is expected that HP could improve mechanical properties of Mg alloys by tuning phase morphology and its composition.

Mg-Li based alloys, because of their super stiffness to weight ratio and excellent cold formability, exhibit more attractive applications of aerospace and aircraft in compared with other ones. According to Mg-Li binary phase diagram,[4] it can be divided into three different ranges depending on Li concentration, i.e., hcp-α, hcp-α+bcc-β, and bcc-β. Wherein duplex phase Mg-Li alloys (hcp-α+bcc-β) containing 5.7–11 wt. % of Li are highly desirable which can provide a optimum combination of mechanical properties. However, low absolute strength is still a critical issue to confine their applications.[5] Generally, two methods are performed to improve strength of Mg-Li based material. One is alloying that a third element, such as Al, Zn, Si, Ag, Cd, or rare earth elements, serves to improve mechanical properties by forming some intermetallic particles.[6] Another is related to grain refinement which induced by various types of deformation treatments.[7,8] Herein, a novel high pressure treatment has been first introduced to improve hardness of Mg-Li alloys. Differing from previous precipitation strengthening and grain refining, this high pressure treatment induces phase transformation, together with the modification of microstructure, resulting in the increment of hardness.

II. EXPERIMENTS

A Mg-7 Li ingot (wt. %, all compositions given thereafter in wt. %) prepared by vacuum induction melting method was machined into samples with 10 mm in diameter and 8 mm in length for HP. The samples were wrapped with Ta foil and then inserted into a BN crucible in a cubic-anvil large-volume press with six rams.[9] The pressure (4 GPa) was added before increasing the temperature. The temperatures varied from 450 to 1150 °C. The time was 120 min. After HP, the samples were quenched to room temperature. Finally, the HP samples were heated (5 °C/min) to 200 °C and reserved for 5 min to release residual stress.

Microhardness was tested with a Vickers hardness tester (HV). The load and the dwelling time were 100 g and 15 s, respectively. A load of 10 kgf and 1 mm ball were performed for Rockwell hardness (RH). Microstructural investigations were performed using scanning electron microscopy (SEM) and transmission electron microscope (TEM). In the case of microstructural observation, the standard procedures including grinding, polishing and etching were applied. The samples were etched in a picral solution to reveal grain boundaries. TEM thin foils were prepared by Ar ion milling in a Fischione system operating at 5 keV at an incidence angle ranging between 7° and 15°. X-ray diffraction (XRD) was carried out on Xpert-Pro diffractometer with Cu Kα radiation in the range from 20° to 80° with 0.2° min^{-1}.

The first-principles calculations were performed using a plane wave pseudopotential approach as implemented in the Vienna *Ab-initio* Simulation Package (VASP) code.[10] Exchange correlation was described by the Perdew–Burke–Ernzerhof generalized gradient approximation.[11] The projector augmented wave[12] method was used to describe Mg and Li. The approximate hcp-Li_5Mg_{31} with a $3 \times 3 \times 2$ supercell and hcp-Li_3Mg_{13} with a $2 \times 2 \times 2$ supercell had been used to study the effects of pressure on enthalpy of hcp-Li_3Mg_{17} and $Li_{0.92}Mg_{4.08}$, respectively.

[a]Author to whom correspondence should be addressed. Electronic mail: pengqiuming@gmail.com

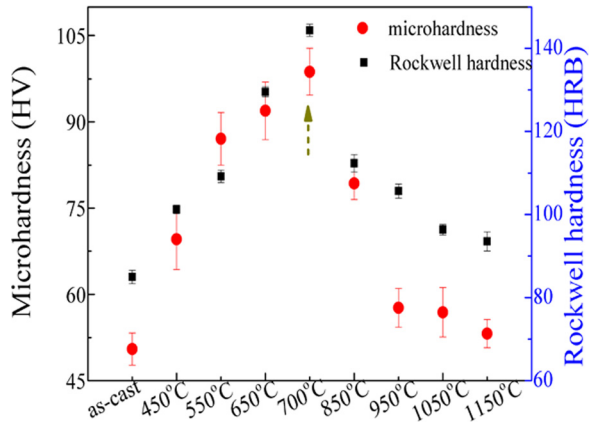

FIG. 1. (a) Effect of high pressure on microhardness and Rockwell hardness.

III. RESULTS AND DISCUSSION

Fig. 1 shows the effect of HP on microhardness and Rockwell hardness of Mg-7 wt. % Li alloy at different temperatures. Both of them reveal the same convex trend in the temperature range between 450 and 1150 °C. Namely, the values increase at initial stage of increasing temperature, and then they decrease after overcoming peak values at 700 °C. For the microhardness, the peak value at 700 °C is 98 HV, which is two times higher than that of as-cast sample.

Fig. 2 shows typical SEM micrographs of different state Mg-7Li alloys. The pristine sample is a typical duplex petal-configuration structure (Fig. 2(a)). The block-shaped phase corresponds to hcp phase. The wide and black grain boundaries are converted into bcc phase with high Li concentration. In contrast, the phase distribution becomes homogeneous after 4 GPa-700 (Fig. 2(b)). The size of hcp phase is reduced. With further increasing the temperature to 1150 °C (Fig. 2(c)), a typical eutectic morphology is observed, indicating a resolidification process occurred under 4 GPa.

Fig. 3 shows XRD patterns of different samples. The pristine Mg-7Li alloy is mostly composed of α and β phases. The β phase corresponds to bcc-Li_3Mg_7 (PDF#65-6742) intermetallic compound. However, α phase contains two stoichiometric compounds, which are hcp-$Li_{0.92}Mg_{4.08}$ (PDF#65-4080) and hcp-Li_3Mg_{17} (PDF#65-5512). Depending on XRD results, the phase relative abundance (PRA) is analysed by Maud software (Fig. 4(a)). The PRA of bcc-Li_3Mg_7 phase in pristine sample is ~0.27, and it reduces to ~0.06 in 4 GPa-700 sample. With further increasing the temperature, the PRA will gradually increase, which corresponds to re-solidification process.

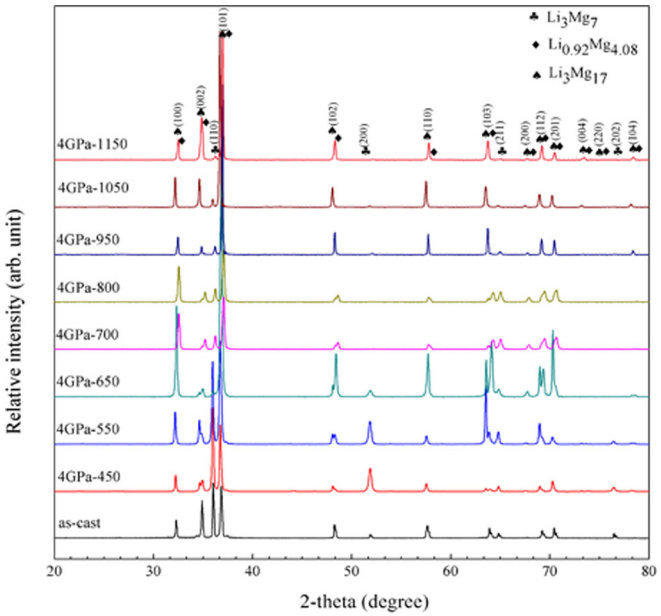

FIG. 3. XRD patterns of different state Mg-7Li alloys.

Regarding to hcp phases, the volume fraction of hcp-$Li_{0.92}Mg_{4.08}$ and hcp-Li_3Mg_{17} compounds fluctuates significantly when the temperature is increased from 450 to 1150 °C. For comparison, the volume ratio (λ) is introduced:[13]

$$\lambda = \frac{\delta_{Li_{0.92}Mg_{4.08}}}{\delta_{Li_3Mg_{17}}}, \quad (1)$$

where δ is volume fraction. The λ also exhibits the convex trend (Fig. 4(b)), which is consistent with the HV and RH results. The value of pristine sample is 0.21, whilst the maximum value of 1.85 is observed in 4 GPa-700 sample.

Fig. 5(a) shows TEM micrograph of as-cast sample. The selected area electron diffraction (SAED) patterns taken from A1 and B1 areas are shown in Figs. 5(d) and 5(e), respectively. Both A1 and B1 are hcp structure, which correspond to [10-10] zone axis, respectively. The lattice parameters of A1 phase are a = 3.182 Å and c = 5.090 Å, whilst those of B1 phase are a = 3.132 Å and c = 5.071 Å. The C phase is confirmed as bcc-Li_3Mg_7 compound. For 4 GPa-700 sample, it consists of two lamellar phases (A2 and B2). The width of B2 phase is measured to be 720 ± 20 nm, which is ~3 times thicker than that of A2 phase. The SAED patterns of the lamellar phases are shown in Figs. 5(f) and 5(g), respectively. Both of them are taken from the [01-11] direction. The *a* and *c* lattices of A2 phase are 3.074 Å and 4.932 Å, whilst the values are 3.041 Å and 4.902 Å for B2

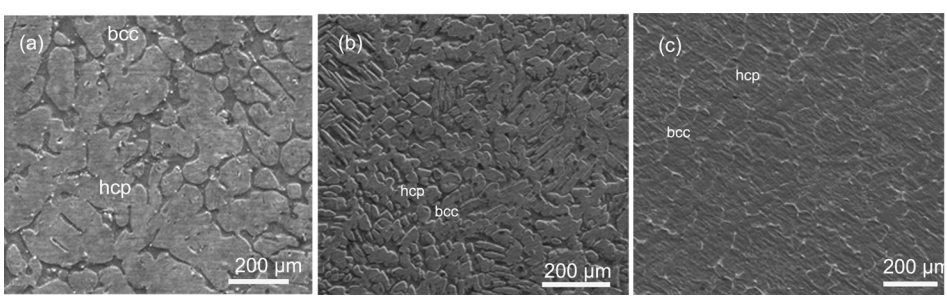

FIG. 2. Typical SEM micrographs of Mg-7Li alloys, (a) as-cast sample; (b) 4 GPa-700; (c) 4 GPa-1150.

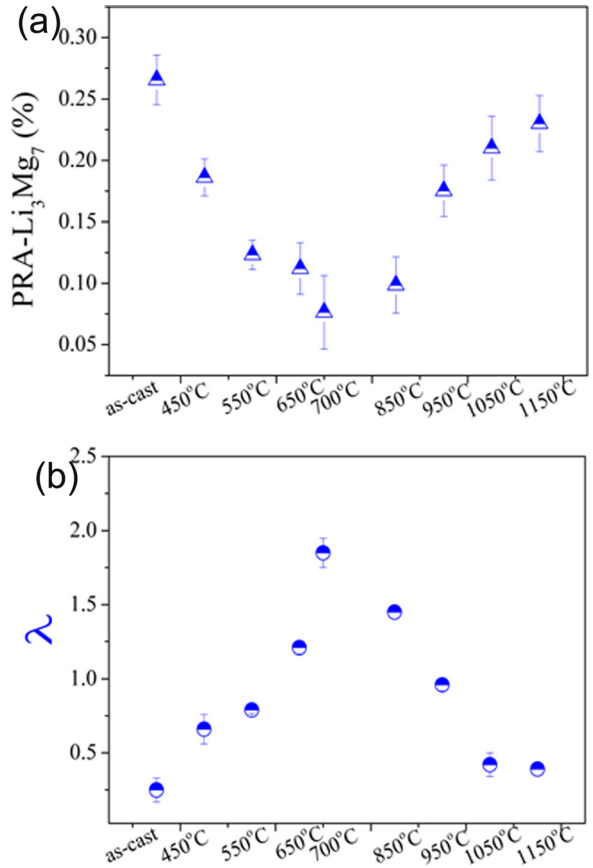

FIG. 4. (a) Effect of temperature on phase relative abundance of bcc-Li_3Mg_7 calculated by Moud software; (b) Effect of temperature on volume ratio ($Li_{0.92}Mg_{4.08}/Li_3Mg_{17}$).

phase. According to the XRD results and previous results,[14,15] it can be confirmed that A1 and A2 phases correspond to hcp-Li_3Mg_{17} phase. The B1 and B2 phases are hcp-$Li_{0.92}Mg_{4.08}$ phase. In addition, as shown in Figs. 5(b) and 5(c), some twins are observed in B2 phase. The $\{10\bar{1}1\}$ compression twins with hundreds of nanometers in the B2 phase are identified along 56° $\langle\bar{1}012\rangle$ (Fig. 5(g)).

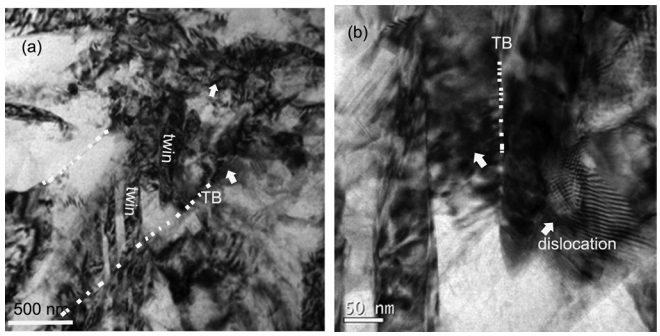

FIG. 6. TEM micrographs of 4 GPa-700 alloy with a true strain of 1%. (a) Some strain areas are observed; (b) local high magnification of (a), where dislocation aggregation is observed in both TBs and twin interiors.

Fig. 6(a) shows the dependence of pressure on formation enthalpy (H). Our results indicate that though both of them are negative, the formation of Li_5Mg_{31} phase is favorable under low pressure. With increasing the pressure, it becomes predominant to form Li_3Mg_{13} phase. The difference in enthalpy ($\Delta H = H_{Li_5Mg_{31}} - H_{Li_3Mg_{13}}$) between two phases (Fig. 6(b)) is decreased as pressure is enhanced, suggesting that the increased pressure is of benefit for phase transformation from Li_3Mg_{17} to $Li_{0.92}Mg_{4.08}$. It is worth noting that the calculation pressure is around 10 GPa, which is greatly decreased with increasing interior temperature.

The improved hardness by HP treatment is mainly associated with the decrease of bcc-Li_3Mg_7 phase. Phase transformation induced the improved mechanical properties has been commonly observed in age hardenable Mg alloys. However, unlike the previous aging process, HP treatment in this work was performed under high pressure and relatively high temperature. Under high pressure, the dislocations tend to pile up at strong barriers owing to the difference in yield stress between two phases, giving rise to very high local stresses.[16] In turn, it can enhance phase transformation. The promotion of phase transformation under HP is also confirmed in preparation of carbon,[17] CaB_4,[18] etc. In this work, the dislocations pile up at the

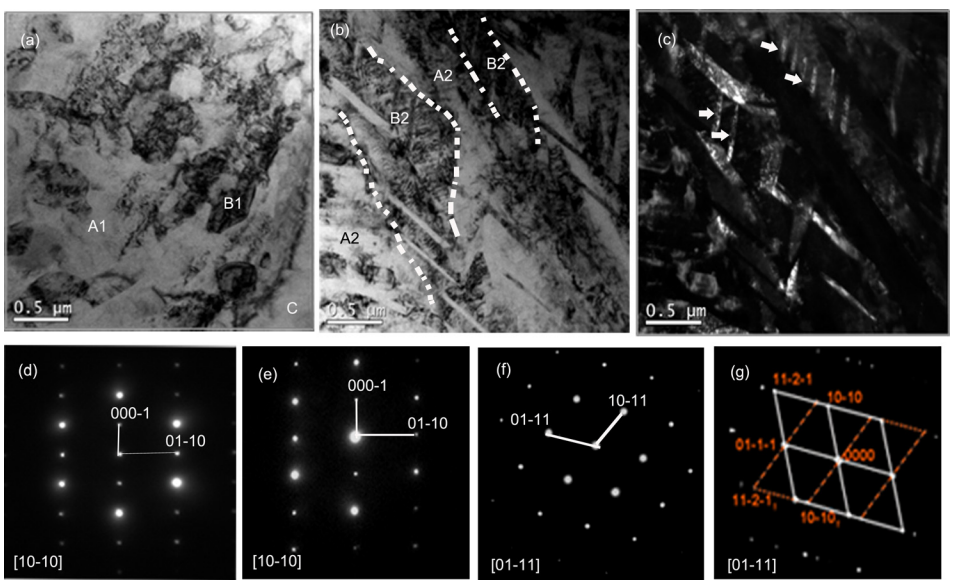

FIG. 5. (a) A typical TEM micrograph of pristine sample; (b) a typical bright-field TEM micrograph of 4 GPa-700 sample;(c) the dark-field micrograph of (b); (d) SAED of A1 phase along [2-1-10] in (a); (e) SAED of B1 phase along [2-1-10] in (a); (f) SAED of A2 phase along [-1101] in (b); (g) SAED of B2 phase along [-1101] in (b).

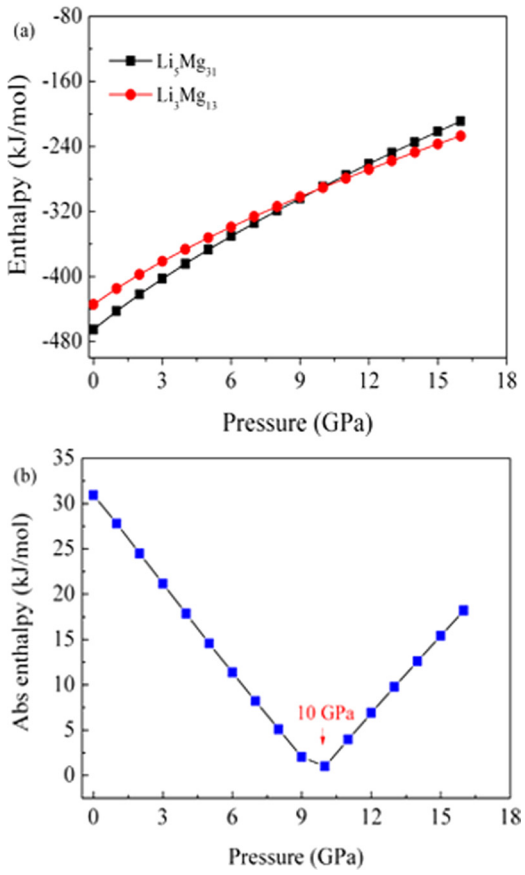

FIG. 7. (a) The enthalpy of Li_5Mg_{31} and Li_3Mg_{13} as a function of pressure; (b) enthalpy difference (ΔH) for Li_5Mg_{31} phase relative to Li_3Mg_{13} structure vs pressure plot.

interface of soft/hard phase such as bcc-Li_3Mg_7/hcp-Li_3Mg_{17} or bcc-Li_3Mg_7/hcp-$Li_{0.92}Mg_{4.08}$. With increasing the temperature, the dislocations will easily cut through a softer bcc phase, leading to its partial dissolution ultimately. As a result, the volume ratio of β phase is reduced, whilst the volume ratio of α phase is increased.

In addition, the presence of $\{10\bar{1}1\}$ compression twins during HP process is also responsible for the improved hardness. According to the model of Estrin and Mecking[19] that the spacing between impenetrable obstacles or grain boundaries decides the mean free path of dislocations, in which the mean free path is determined by both dislocation-dislocation interaction and barriers in grain or twin boundaries (TBs). Since the formation of twins subdivide grain to more twin boundaries, which offers additional barriers to dislocation movement. As shown in Fig. 7(a), a large number of deformed areas are observed in grain/TBs. Under higher magnification (Fig. 7(b)), the tangled dislocations are observed both grain boundaries and twin interiors, demonstrating that the presence of compression twins plays an effective role in prohibiting dislocation movement. On the other hand, the formation of twins in Mg alloys generally results in the variation of grain size.[20] Namely, the interior of twins provides an effective nucleation for forming fine grains during the deformation. Thus, the mechanical properties can be improved correspondingly in terms of Hall-Petch hardening.[20]

IV. CONCLUSION

The high pressure thermal-mechanical treatment is an effective approach to improve hardness of a duplex Mg-7 wt. % Li alloy. Both the reduced volume fraction of bcc-Li_3Mg_7 phase and the presence of $\{10\bar{1}1\}$ compression twins in hcp-$Li_{0.92}Mg_{4.08}$ phase are essential reasons for the improved hardness. The calculation indicates that phase transformation occurs under 10 GPa spontaneously. However, the experimental results reveal that the critical pressure of phase transformation sharply decreases with increasing temperature.

ACKNOWLEDGMENTS

This research was supported by NSFC (Nos. 51101142, 50821001, and 51102206), New Century Excellent Talents in University of Ministry of Education of China (NCET-12-0690), and Heibei province scientific program (Nos. 13961002D and Y2012019).

[1]Y. Tian, B. Xu, D. Yu, Y. Ma, Y. Wang, Y. Jiang, W. Hu, C. Tang, Y. Gao, K. Luo, Z. Zhao, L. M. Wang, B. Wen, J. He, and Z. Liu, Nature **493**, 385 (2013).
[2]A. Kamegawa, Y. Goto, H. Kakuta, H. Takamura, and M. Okada, J. Alloys Compd. **408–412**, 284 (2006).
[3]J. C. Jie, C. M. Zou, H. W. Wang, B. Li, and Z. J. Wei, Scr. Mater. **64**, 588 (2011).
[4]M. M. Avedesian and H. Baker, *ASM Specialty Handbook: Magnesium and Magnesium Alloys* (ASM International, Materials Park, OH, 1999).
[5]W. Gasior, Z. Moser, W. Zakulski, and G. Schwitzgebel, Metall. Mater. Trans. A. **27**, 2419 (1996).
[6]W. A. Counts, M. Friák, D. Raabe, and J. Neugebauer, Adv. Eng. Mater. **12**, 1198 (2010).
[7]B. Srinivasarao, A. P. Zhilyaev, I. Gutiérrez-Urrutia, and M. T. Pérez-Pradoa, Scr. Mater. **68**, 583 (2013).
[8]T. Liu, Y. D. Wang, S. D. Wu, R. Lin Peng, C. X. Huang, C. B. Jiang, and S. X. Li, Scr. Mater. **51**, 1057 (2004).
[9]S. Wang, D. He, W. Wang, and L. Lei, High Pressure Res. **29**, 806 (2009).
[10]G. Kresse and J. Hafner, Phys. Rev. B **47**, 558 (1993).
[11]J. P. Perdew, K. Burke, and M. Ernzerhof, Phys. Rev. Lett. **77**, 3865 (1996).
[12]P. E. Blöchl, Phys. Rev. B **50**, 17953 (1994).
[13]R. A. Young and D. B. Wiles, J. Appl. Crystallogr. **15**, 430 (1982).
[14]D. Hardie and R. N. Parkins, Philos. Mag. **4**, 815 (1959).
[15]F. H. Herbstein and B. L. Averbach, Acta Metall. **4**, 407 (1956).
[16]V. I. Levitas, J. Mech. Phys. Solids **45**, 923 (1997).
[17]Q. Li, Y. Ma, A. R. Oganov, H. Wang, H. Wang, Y. Xu, T. Cui, H. K. Mao, and G. Zou, Phys. Rev. Lett. **102**, 175506 (2009).
[18]Z. Liu, X. Han, D. Yu, Y. Sun, B. Xu, X. F. Zhou, J. He, H. T. Wang, and Y. Tian, Appl. Phys. Lett. **96**, 031903 (2010).
[19]Y. Estrin and H. Mecking, Acta Metall. **32**, 57 (1984).
[20]S. G. Hong, S. H. Park, and C. S. Lee, Acta Mater. **58**, 5873 (2010).